

Controlling size and magnetic properties of Fe₃O₄ clusters in solvothermal process

Sergio I. Uribe Madrid¹, Umapada Pal*¹ and Félix Sánchez-De Jesús²

¹Instituto de Física, Benemérita Universidad Autónoma de Puebla,
Apdo. Postal J-48, Puebla, Pue. 72570, Mexico

²Area Academica de Ciencias de la Tierra y Materiales, Universidad Autónoma del Estado de Hidalgo,
Carr. Pachuca-Tulancingo Km. 4.5, 42184 Pachuca, Hidalgo, Mexico

(Received August 5, 2014, Revised January 13, 2015, Accepted January 14, 2015)

Abstract. Magnetite nanoparticles (MNPs) of different sizes were synthesized by solvothermal process maintaining their stoichiometric composition and unique structural phase. Utilizing hydrated ferric (III) chloride as unique iron precursor, it was possible to synthesize sub-micrometric magnetite clusters of sizes in between 208 and 381 nm in controlled manner by controlling the concentration of sodium acetate in the reaction mixture. The sub-micrometer size nanoclusters consist of nanometric primary particles of 19 - 26.3 nm average size. The concentration of sodium acetate in reaction solution seen to control the final size of primary MNPs, and hence the size of sub-micrometric magnetite nanoclusters. All the samples revealed their superparamagnetic behavior with saturation magnetization (M_s) values in between 74.3 and 77.4 emu/g. The coercivity of the nanoclusters depends both on the size of the primary particles and impurity present in them. The mechanisms of formation and size control of the MNPs have been discussed.

Keywords: magnetite nanoclusters; solvothermal synthesis; size control; magnetic properties

1. Introduction

Synthesis of magnetite nanoparticles (MNPs) has attracted much attention in recent years due to their wide range of applications in different fields such as in magnetic recording (Dai *et al.* 2010), water splitting (Parkinson *et al.* 2011), magnetic resonance imaging (MRI) (Jun *et al.* 2005), targeted drug delivery (Roullin *et al.* 2002), catalysis (Jung *et al.* 2008), etc. However, for each of these applications, MNPs of specific size range, specific magnetic behavior, and surface characteristics are required. For example, MNPs of 10-50 nm size range with superparamagnetic behavior are required for MRI applications (Huh *et al.* 2005, Haw *et al.* 2010, Song *et al.* 2011). On the other hand, for targeted drug delivery and biomedical applications, apart from superparamagnetic nature, MNPs of 100-300 nm size range with high saturation magnetization have been utilized (Berry *et al.* 2003). Although for therapeutic applications, MNPs of a wider size range (5-1200 nm) could be utilized depending on specific usage, the performance of most of the MNP-based drug delivery systems depends on the size and shape of MNPs (Devadasu *et al.* 2013).

*Corresponding author, Professor, E-mail: upal@ifuap.buap.mx

On the other hand, principal characteristics of MNPs required for their catalytic applications are their porosity and high specific surface area (Zhu *et al.* 2011). Most of these characteristics of MNPs depend strongly on the method employed for their synthesis (Iida *et al.* 2007).

Several techniques like thermal decomposition (Park *et al.* 2004), micro-emulsion (Ha *et al.* 2008), sonochemical (Wu *et al.* 2007), sol-gel (Larumbe *et al.* 2012), polyol (Cai and Wan 2007), co-precipitation (Zhao *et al.* 2006) and hydrothermal/solvothermal (Haw *et al.* 2010), have been employed to synthesize MNPs. While every method has its advantages and disadvantages, the latter two are most popular as they produce crystalline MNPs with controlled size and morphology in reasonable cost and good yield. In addition, no post-synthesis heat treatment is required for the MNPs produced by these techniques, especially for the MNPs prepared by hydrothermal/solvothermal technique; which made this method highly desirable as any post-synthesis heat treatment might result in particle agglomeration (Devadasu *et al.* 2013), along with a change in their magnetic behaviors.

In thermal decomposition synthesis, frequently iron pentacarbonyl (FeCO_5) is used as iron precursor (Park *et al.* 2005), which is toxic and expensive. Some researchers (Chin *et al.* 2011) have also reported the use of non-toxic organic precursors for thermal decomposition. However, in both the cases, synthesized MNPs were below 10 nm size. Using sonochemical method, Marchegiani *et al.* (2012) could synthesize MNPs in 10 - 30 nm size range, with saturation magnetization lower than 75 emu/g. On the other hand, using sol-gel and micro-emulsion techniques, Larumbe *et al.* (2012) and Liu *et al.* (2004) could synthesize MNPs of about 7.5 and 10 nm average size, respectively. However, Cai and Wan (2007) could tune the size of MNPs in between 5 and 40 nm in their polyol synthesis process.

As can be noted, while thermal decomposition, sol-gel and micro-emulsion techniques can produce homogeneous MNPs of sizes below 10 nm, sonochemical and polyol synthesis can produce MNPs of relatively bigger sizes, although the size dispersion in the MNPs produced by latter methods is often higher.

The solvothermal process normally produces MNPs of bigger sizes in the range of 250-400 nm, mostly as agglomerate of smaller particles of 9-30 nm sizes, due to their high surface energy and strong effective surface tension. As these bigger agglomerated clusters contain closely packed MNPs of smaller sizes, they manifest strong superparamagnetic behaviors and high saturation magnetization, which are essential requirements for several biomedical applications. As has been stated earlier, MNPs of a wide size-range are useful for biomedical applications depending on their specific usage. Therefore, synthesis of superparamagnetic MNP clusters with controlled size and size dispersion in the 200-500 nm size range is a big challenge for their biomedical and therapeutic applications. Using solvothermal process, recently Kumar *et al.* (2013) prepared monodispersed MNPs of different sizes by varying the concentration of iron precursor in reaction mixture. Using dodecylamine as surfactant and ethylene glycol as solvent, Chen *et al.* (2012) could prepare relatively bigger MNPs (300-700 nm average sizes) through solvothermal process. Through solvothermal process, Xuang *et al.* (2011) could prepare MNPs of wider size range (50-200 nm), utilizing poly (acrylic acid) spheres as template. However, the saturation magnetization M_s of their nanoparticles were relatively low. Solvothermal synthesis of highly monodispersed superparamagnetic MNPs of about 300 nm average size and $M_s > 80$ emu/g has been reported by Xu *et al.* (2010) using sodium acetate (NaAc) as precipitating agent and ethylene glycol (EG) as solvent. Although several routes and a variety of solvents, surfactants, and precipitating agents have been utilized to synthesize MNPs of different sizes and different surface properties, controlling their size, dispersion, and magnetic behaviors remain a great challenge for their practical

applications.

In this article, we report the synthesis of hydrophilic MNPs through a low temperature sodium acetate mediated solvothermal process, where both their size and magnetic behaviors could be controlled by controlling reaction conditions. We demonstrate that the size of the magnetite clusters can be controlled in between 208 and 381 nm using single iron (III) chloride precursor, just by controlling the molar ratio of iron precursor and sodium acetate in the reaction mixture.

2. Materials and methods

2.1 Chemicals & solvent

Ferric chloride hexahydrate ($FeCl_3 \cdot 6H_2O$, 97%) and anhydrous sodium acetate (NaAc) (CH_3COONa , 99.9%) were obtained from Sigma-Aldrich, USA. Ethylene glycol (EG, $C_2H_6O_2$, 99.7 %) was purchased from J. T. Baker, Mexico. *E*-pure deionized (DI) water ($\rho > 18.2 \Omega \cdot cm$) was used as solvent for washing. All the chemicals were of analytical grade and used as received.

2.2 Solvothermal synthesis of Fe_3O_4 nanoparticles

In a typical synthesis process, first a 0.6M $FeCl_3 \cdot 6H_2O$ solution was prepared by dissolving 1.621 g of $FeCl_3 \cdot 6H_2O$ in 10 mL of EG. The solution was added to 40 mL of EG in a two-necked round bottom flask under Ar flow and magnetic agitation. After 30 min of stirring, 10 mL of sodium acetate solution of a particular molar concentration (0.9 M - 1.5 M, using EG as solvent, M represents mol/L) was added to the previous mixture under vigorous magnetic stirring. The stirring process was continued for another 3 h and then the mixture was transferred to a Teflon-lined stainless steel autoclave and heated at 190°C for 24 h. Finally the autoclave was cooled down to room temperature and the product was magnetically separated, washed with water and ethanol several times, dried at 65°C for 12 h and stored under Ar atmosphere. All the synthesized samples (MNPs) were highly hydrophilic, and therefore, could be dispersed in water very easily.

2.3 Characterization of MNPs

Field emission high-resolution scanning electron microscopy (FE-HRSEM; Zeiss Auriga 3916) and high resolution transmission electron microscopy (HRTEM; JEM-ARM200F) were used to determine the size and morphology of the synthesized nanoclusters. Crystalline phase of the nanostructures was studied by X-ray diffraction (XRD) using the CuK_{α} emission ($\lambda = 1.5406 \text{ \AA}$) of a Bruker Discover D8 diffractometer. Room temperature Raman spectra of the samples were collected using a microRaman system (Horiba JOBIN-YVON spectrophotometer) utilizing a He-Ne laser ($\lambda = 532.6 \text{ nm}$) excitation source and a thermoelectrically cooled charge-coupled device (CCD). A MicroSense EV7 vibrating sample magnetometer (VSM) was used to record the room temperature (RT) magnetization curve of the nanostructures. To determine the specific surface area of the magnetite clusters, their N_2 adsorption-desorption isotherms at 77K were recorded using Belsorp-Mini II (BEL Japan, Inc) analyzer. The samples were degassed at 150°C for 6 h in vacuum prior to the measurements.

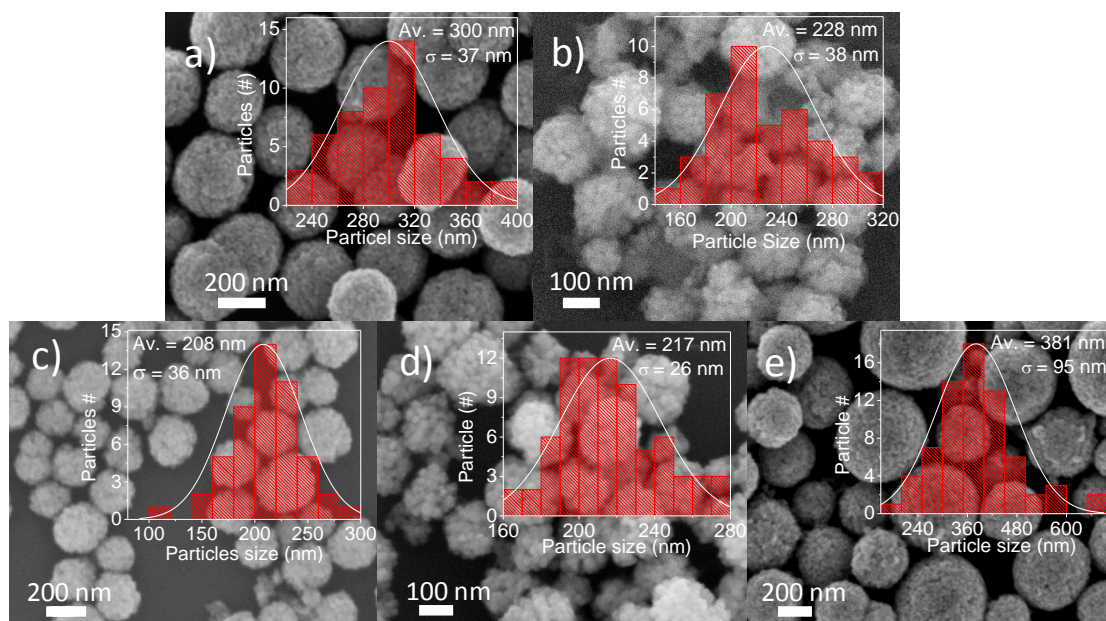


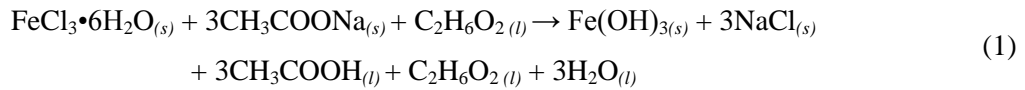
Fig. 1 Typical SEM images of Fe_3O_4 clusters prepared with (a) 0.9M, (b) 1.05M, (c) 1.2M, (d) 1.35M, (e) 1.5M concentrations of sodium acetate in the reaction mixture. The insets present the size distribution histograms of the corresponding magnetite clusters

3. Results and discussion

Fig. 1 shows the typical SEM images of the magnetite samples prepared at different sodium acetate concentrations. All the samples revealed the formation of spherical clusters of sub-micrometer sizes made of nanometer size primary particles, indicating their formation through agglomeration of smaller units. From the size distribution histograms of the clusters (presented as insets of the corresponding SEM images), it is clear that their final size depends on the concentration of sodium acetate in reaction mixture (Fig. 2). Using high-resolution SEM images of the clusters, the average size of the constituting smaller particles (primary particles here after) in the clusters of each sample could be estimated (see Fig. 3 and Fig. S1-S5 of the supplementary information). As can be seen, both the average size of the sub-micrometric clusters and average size of the nanometric primary particles vary with the concentration of sodium acetate in reaction mixture. While the size variation of the primary particles with the variation of sodium acetate concentration can be understood from the mechanism of reactions occurred during the solvothermal process (discussed later), the size variation of the sub-micrometer clusters is seen to depend on the size of primary particles. As can be seen from Figs. 2, 3, the size of the sub-micrometer clusters and their constituting primary particles vary oppositely. As the surface energy of smaller primary particles is higher than the bigger ones, the probability of their agglomeration is higher; and hence, a larger number of smaller primary particles agglomerate to form bigger clusters, and vice versa. However, agglomeration of magnetic particles in solution containing surfactant is controlled not only by their surface energy, but also by van der Waals, electrostatic, and magnetic-dipole forces, along with non-DLVO (Derjaguin-Landau-Verwey-Overbeek) steric repulsion (Ching *et al.* 2002).

Although there exist many reports on the reaction mechanism involved in the formation of magnetite in the thermal decomposition (Ravikumar *et al.* 2011), co-precipitation (Mascolo *et al.* 2013), polyol (Cha *et al.* 2013) and other processes, the reaction mechanism involved in solvothermal synthesis of MNPs is not yet clear. Considering the reducing behavior of EG at high temperatures in the polyol process (Blin *et al.* 1989), the reaction involved in the solvothermal process while using FeCl₃•6H₂O as unique iron precursor can be expressed as follows.

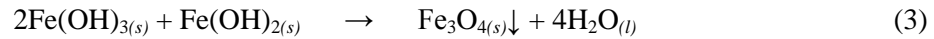
Initially when we dissolve iron (III) chloride and sodium acetate in ethylene glycol, the Fe(OH)₃ is produced following the reaction



On heating the reaction mixture at high temperature (190°C, which is close to the boiling point of ethylene glycol, 197°C), ethylene glycol acts as a reducing agent to produce iron (II) hydroxide



Finally, these iron (III) and iron (II) hydroxides react in 2:1 molar ratio at higher temperature (190°C) to form magnetite nanostructures following the reaction



In fact, the concentration of sodium acetate in reaction mixture determines the size of primary particles, and hence the final size of the magnetite clusters, as has been proposed by Yu and Kwak (2011) for their solvothermally synthesized metal ferrites. A higher concentration of sodium acetate in reaction mixture produces iron (III) hydroxide in higher concentration, which during solvothermal process reacts with iron (II) hydroxide, producing magnetite nanostructures with yield in between 6-50% (Fig. 3). While the production yield of magnetite increases linearly with the increase of sodium acetate concentration in the reaction mixture, after a critical concentration, the size of the primary MNPs decreases (Fig. 3).

The size reduction of the primary MNPs at very high concentrations of sodium acetate is expected, as the production of Fe(OH)₃ is very high for high sodium acetate concentration. While both the nucleation and growth rate of primary MNPs increase initially on increasing the Fe(OH)₃ in the reaction mixture, and hence increasing their average size and the production yield. Presence of excessive Fe(OH)₃ in the reaction mixture (in excess of Fe³⁺ ions) will generate a dielectric double-layer around the primary particles, restricting their further growth. Therefore, the used sodium acetate not only acts as a precipitating agent, but also as protecting agent of the primary MNPs. As both the nucleation and growth rate of the primary particles are very high for a high sodium acetate concentration, they become more dispersed in size, as has been observed in our SEM analysis (Fig. 2). However, generation of Fe(OH)₃ in excess in the reaction mixture for high sodium acetate concentration (which form the protecting layer around the primary particles) improve their size dispersion by restricting further growth.

The magnetization curves (M vs. H curves) for the samples synthesized at 0.9, 1.2, and 1.5M concentrations of sodium acetate are shown in Fig. 4. All the samples revealed superparamagnetic behavior with saturation magnetization (*M_s*) varying in-between 74.3 and 77.4 emu/g. The values are higher than the *M_s* values reported by several research groups for the MNPs prepared by different synthesis techniques (Iida *et al.* 2007, Park *et al.* 2004, Zhao *et al.* 2006, Sun *et al.* 2009). It should be noted that the *M_s* reported for bulk magnetite is about 92 emu/g (Han *et al.* 1994). Though the saturation magnetization as high as 81 emu/g has been reported by some researchers

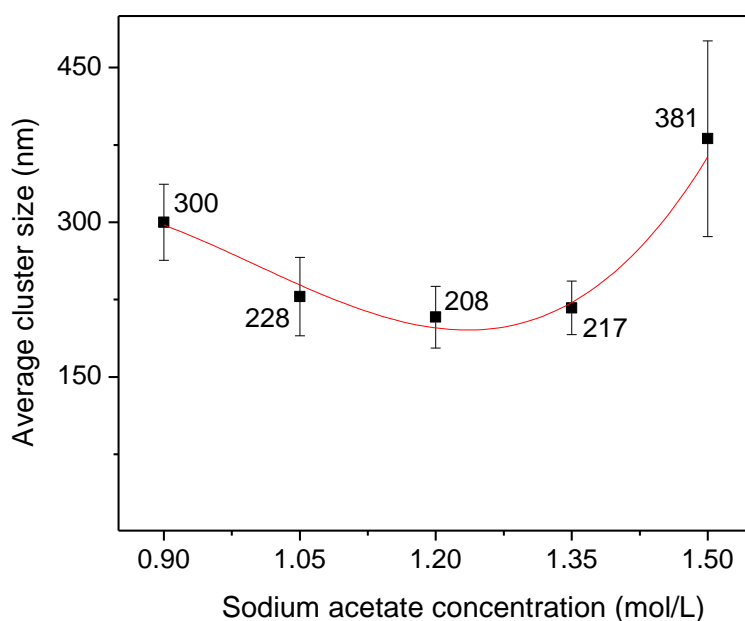


Fig. 2 Variation of magnetite cluster size with the concentration of sodium acetate in reaction mixture

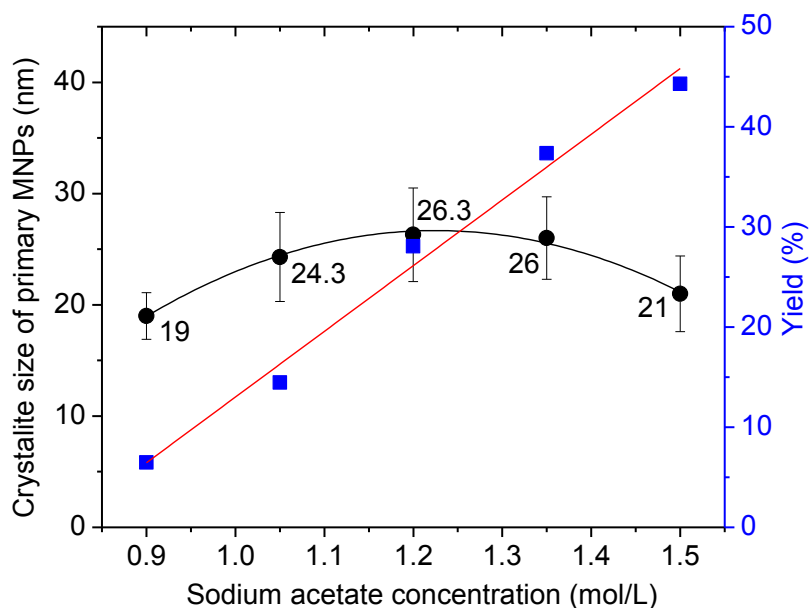


Fig. 3 Variation of production yield and average crystallite size of the primary MNPs with the variation of sodium acetate concentration in the reaction mixture

(Hu *et al.* 2009, Deng *et al.* 2005, Xu *et al.* 2010, Deng *et al.* 2008) for the MNPs synthesized by hydrothermal/solvothermal technique, their process temperature was higher (200°C) than the temperature (190 °C) we used for solvothermal treatment. The MNPs prepared at higher hydrothermal/solvothermal temperature have better crystallinity. As can be seen from the HRTEM

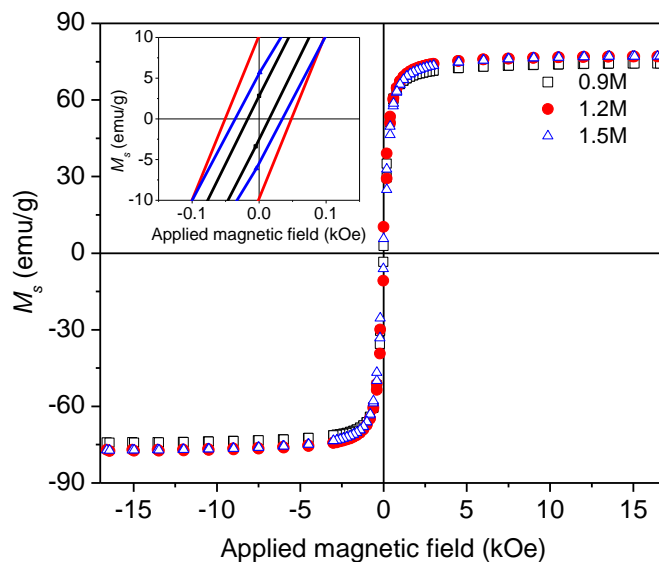


Fig. 4 Magnetization curves for the magnetite clusters synthesized with sodium acetate concentration of 0.9M, 1.2M and 1.5M in the reaction mixture

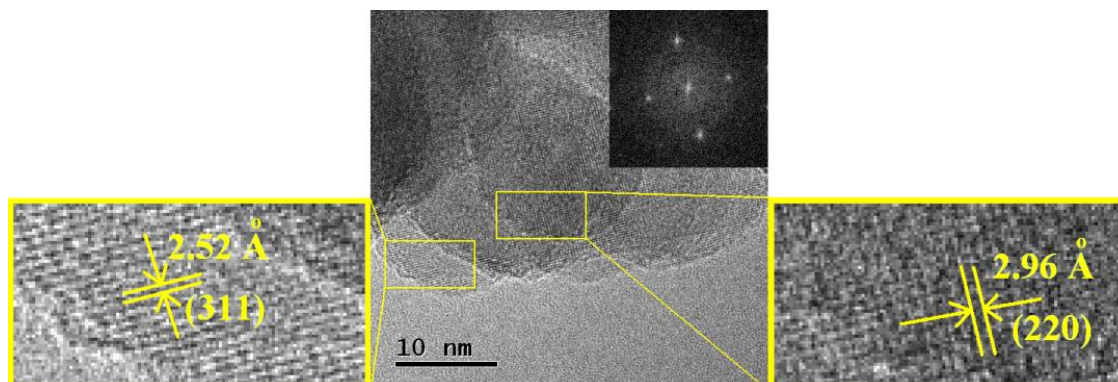


Fig. 5 Representative HRTEM images of a magnetite cluster synthesized with sodium acetate concentration of 1.2M. Clear lattice fringes in the high-resolution image clearly demonstrate good crystallinity of the primary MNPs

image of our samples presented in Fig. 5, all the primary MNPs in the clusters are highly crystalline, though not of single-crystalline nature. Therefore, we believe, the lower M_s values in our samples is associated to arbitrary orientation of the magnetic domains and the presence of NaCl as impurity formed during the reaction, which was not removed completely during washing. While a higher M_s for the MNPs grown at higher temperature is well known (Guardia *et al.* 2007), the effect of NaCl impurity was verified by measuring the EDS spectra of a sample after repeated washing (Fig. S6 of SI). As can be seen from the inset of the Fig. 4 and Table 1, the coercivity of our samples prepared with different concentrations of sodium acetate vary in between 15 and 49 Oe. Though most of the published works do not report the coercivity values for their synthesized MNPs, Zhu and Diao (2011) have reported a coercivity of 35.5 Oe for their magnetite clusters

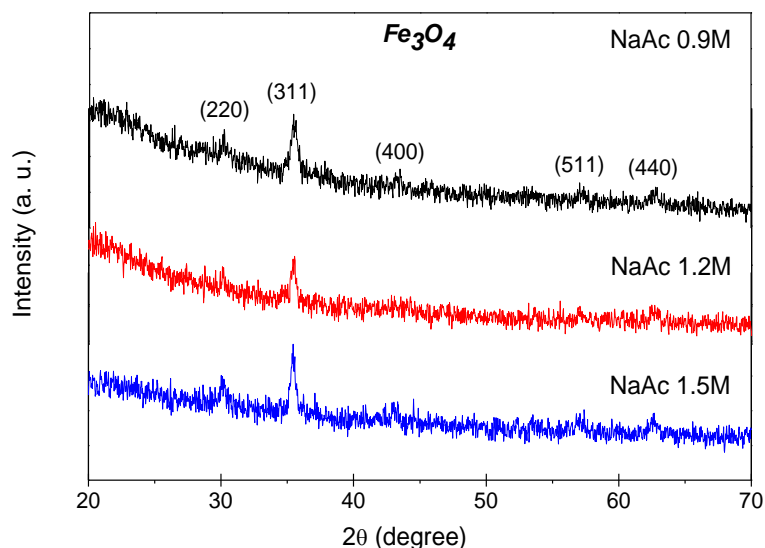


Fig. 6 XRD patterns of the magnetite clusters prepared with different concentrations of sodium acetate in the reaction mixture

Table 1 Particle and grain size variation of magnetite nanoparticles grown at different synthesis conditions

Sample	Sodium acetate conc. (mol/L)	SEM estimated av. cluster size (nm)	HRSEM estimated av. primary particle size (nm)	XRD estimated av. grain size (nm)	M_s (emu/g)	H_c (Oe)
Fe₃O₄	0.9	300	19	14	74.3	15
	1.05	228	24.3	15.4	77.3	27
	1.2	208	26.3	20.5	77	48
	1.35	217	26	18.1	76	49
	1.5	381	21	17.8	77.4	35

consisting 12 nm primary nanoparticles. Again, the fluctuation of coercivity in our samples can be associated to the presence of NaCl as impurity.

Fig. 6 shows the XRD patterns of the Fe₃O₄ clusters prepared at different sodium acetate concentrations. As can be seen, all the samples revealed diffraction peaks associated to magnetite in cubic phase (PDF #89-0691). The average crystallite size in the clusters was estimated through Debye-Scherrer equation ($D=0.9\lambda/\beta\cos\theta$) using the most intense (311) diffraction peak of the samples (Table 1), where D is the crystallite size, λ is the radiation wavelength ($\text{CuK}\alpha=0.15406$ nm), θ is the diffraction peak angle, and β is the full width at half maximum (FWHM) of the diffraction peak. From the Table 1, we can see that the crystallite size of the samples depend strongly on the concentration of sodium acetate, which vary in between 19 and 26.3 nm.

We must recognize that the XRD pattern of standard Fe₃O₄ (magnetite) is very similar to the standard γ -Fe₂O₃ (maghemite) sample, with only difference of two low intensity peaks appearing at about 23.7 and 26.1 degrees in the later. However, these diffraction peaks are not present in our samples (Fig. 6). However, as the intensity of these peaks in XRD pattern of maghemite generally appear in very low intensities, we cannot exclude the possibility of the presence of γ -Fe₂O₃ in our samples considering their XRD patterns only. To verify the phase pure nature of our samples, we

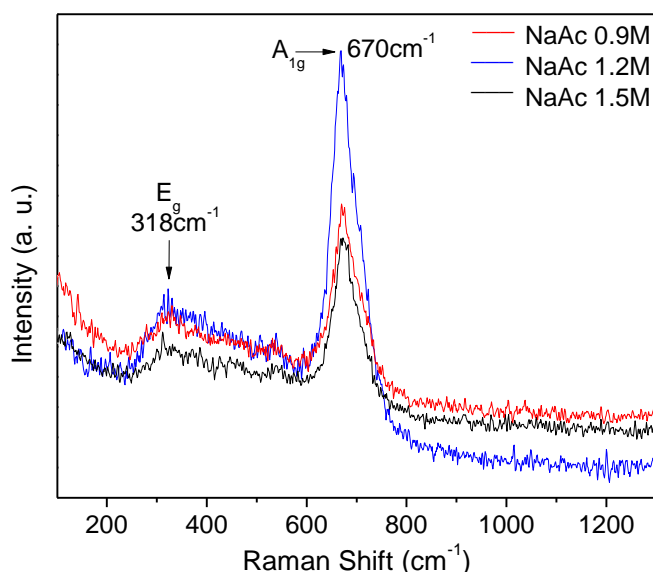


Fig. 7 Room temperature micro Raman spectra of the magnetite clusters prepared at different sodium acetate concentrations in reaction mixture

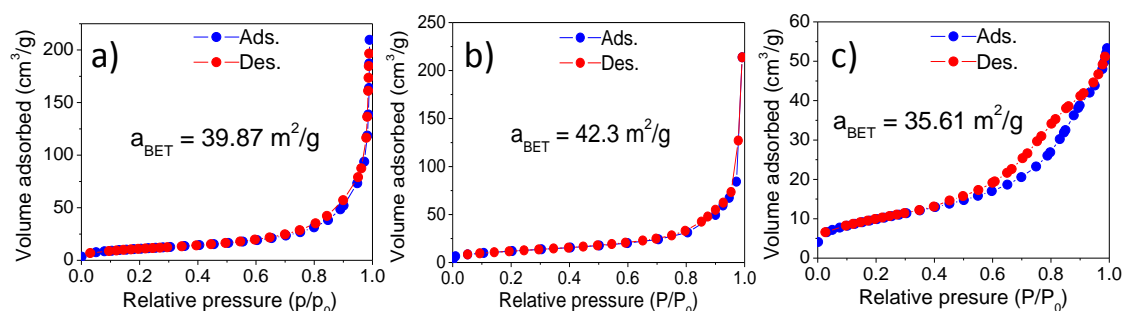


Fig. 8 N_2 adsorption–desorption isotherms of the magnetite clusters prepared with (a) 0.9M, (b) 1.2M, (c) 1.5M concentrations of sodium acetate in the reaction mixture

recorded their Raman spectra at room temperature.

To confirm the structural phase of the synthesized nanostructures, we analyzed all the samples by microRaman spectroscopy at room temperature (Fig. 7). All the samples revealed an intense peak centered around 670 cm^{-1} , which corresponds to the A_{1g} mode (Fe-O symmetric stretching) of pure Fe_3O_4 . The low intensity Raman peak appeared at about 318 cm^{-1} corresponds to the E_g mode (Fe-O symmetric bending) of Fe_3O_4 (Degiori *et al.* 1987, Legodi and Waal 2007). Absence of any Raman peak near 700 , 500 or 350 cm^{-1} , which correspond to the phonon modes of $\gamma\text{-Fe}_2\text{O}_3$ (De Faria *et al.* 1997), indicates all the samples we prepared are of pure Fe_3O_4 phase. The observation is also in good agreement with the proposed mechanism that favors the formation of magnetite over the $\gamma\text{-Fe}_2\text{O}_3$ nanoparticles in the presence of excess EG, which guarantee the reduction of Fe^{3+} to Fe^{+2} keeping their concentration ratio 2:1 in the reaction mixture necessary for producing magnetite.

The specific surface area of the porous magnetite clusters prepared with 0.9, 1.2, and 1.5 M

concentrations of sodium acetate have been studied by recording their N₂ adsorption-desorption isotherms at 77K (Fig. 8). From Fig. 8, we can see that all the samples revealed characteristics of both type II and type IV porous materials (IUPAC classification) (Sing *et al.* 1985). As the magnetite clusters are formed by the interconnected primary particles of about 20 nm size, without following any order, both type II and type IV characteristics of the isotherms indicate the mixed macro- and mesoporous nature of the samples with inhomogeneous pore size distribution. The BET estimated specific surface area of the clusters prepared with 0.9, 1.2, and 1.5 M concentrations of sodium acetate were of 39.87, 42.3 and 35.61 m²/g, respectively.

4. Conclusions

In summary, we could synthesize magnetite nanoclusters of different sizes in controlled manner through solvothermal process, maintaining their stoichiometric composition and unique structural phase. By varying the concentration of precipitating agent (sodium acetate) in the reaction mixture, the size and morphology of the nanoclusters could be controlled in between 208 and 381 nm, utilizing FeCl₃•6H₂O as unique iron precursor and ethylene glycol as solvent. The sub-micron size magnetite clusters are formed by the agglomeration of smaller primary nanoparticles of 19-26.3 nm sizes. While the size of sub-micrometer magnetite clusters depends on the average size of primary nanoparticles, their surface energy and aggregation behaviors, their magnetic properties depend on the size of primary particles and impurity content. While an increase of sodium acetate concentration in the reaction mixture enhances the production yield of the magnetite clusters linearly, sodium acetate concentration higher than an optimum value reduces the size of primary nanoparticles.

Acknowledgements

The work has been carried out with the financial helps extended by VIEP-BUAP and CONACyT, Mexico, through the project grants # VIEP/EXC/2014 and CB-2010/151767, respectively. Authors are thankful to the Advance Electronic Nanoscopy Laboratory, CINVESTAV, Mexico, for extending SEM facility.

References

- Berry, C.C. and Curtis, A.S.G. (2003), "Functionalisation of magnetic nanoparticles for applications in biomedicine", *J. Phys. D: Appl. Phys.*, **36**(13), R198-R206.
- Blin, B., Fievet, F., Beaupere, D. and Filglarz, M. (1989), "Oxydation duplicative de l'éthylène glycol dans un nouveau procédé de préparation de poudres métalliques", *Nouv. J. Chim.*, **13**, 67-72.
- Cai, W. and Wan, J. (2007), "Facile synthesis of superparamagnetic magnetite nanoparticles in liquid polyols", *J. Colloid Interf. Sci.*, **305**(2), 366-370.
- Cha, J., Lee, J.S., Yoon, S.J., Kim, Y.K. and Lee, J.K. (2013), "Solid-state phase transformation mechanism for formation of magnetic multi-granule nanoclusters", *RSC Adv.*, **3**(11), 3631-3637.
- Chen, Y., Xia, H., Lu, L. and Xue, J. (2012) "Synthesis of porous hollow Fe₃O₄ beads and their application in lithium ion batteries", *J. Mater. Chem.*, **22**, 5006-5012.
- Chin, S.F., Pang, S.C. and Tan, C.H. (2011), "Green synthesis of magnetite nanoparticles (via thermal

- decomposition method) with controllable size and shape”, *J. Mater. Environ. Sci.*, **2**(3) 299-302.
- Ching, C.J., Yiacomini, S. and Tsouris, C. (2002), “Agglomeration of magnetic particles and breakup of magnetic chains in surfactant solutions”, *Coll. Surf. A: Physicochem. Eng. Aspect.*, **204**(1-3), 63-72.
- De Faria, D.L.A., Venancio Silva, S. and de Oliveira, M.T. (1997), “Raman microspectroscopy of some iron oxides and oxyhydroxides”, *J. Raman Spectrosc.*, **28**(11), 873-878.
- Dai, Q., Berman, D., Virwani, K., Frommer, J., Jubert, P.O., Lam, M., Topuria, T., Imaino, W. and Nelson, A. (2010), “Self-assembled ferrimagnet-polymer composites for magnetic recording media”, *Nano Lett.*, **10**(8), 3216-3221.
- Degiorgi, L., Blatter-Mörke, I. and Wachter, P. (1987), “Magnetite: phonon modes and the Verwey transition”, *Phys. Rev. B*, **35**(11), 5421-5424.
- Deng, H., Li, X., Peng, Q., Wang, X., Chen, J. and Li, Y. (2005), “Monodisperse magnetic single-crystal ferrite microspheres”, *Angew. Chem. Int. Ed.*, **44**(18), 2782-2785.
- Deng, Y., Qi, D., Deng, C., Zhang, X. and Zhao, D. (2008), “Superparamagnetic high-magnetization microspheres with a Fe₃O₄@SiO₂ core and perpendicularly aligned mesoporous SiO₂ shell for removal of microcystins”, *J. Am. Chem. Soc.*, **130**(1), 28-29.
- Devadasu, V.R., Bhardwaj, V. and Ravi Kumar, M.N.V. (2013), “Can controversial nanotechnology promise drug delivery?”, *Chem. Rev.*, **113**(3), 1686-1735.
- Guardia, P., Batlle-Brugal, B., Roca, A.G., Iglesias, O., Morales, M.P., Serna, C.J., Labarta, A. and Batlle, X. (2007), “Surfactant effects in monodisperse magnetite nanoparticles of controlled size”, *J. Magn. Magn. Mater.*, **316**(2), e756-e759.
- Ha, N.T., Hai, N.H., Luong, N.H., Chau, N. and Chinh, H.D. (2008), “Effects of the conditions of the microemulsion preparation on the properties of Fe₃O₄ nanoparticles”, *VNU J. Sci. Natl. Sci. Technol.*, **24**, 9-15.
- Han, D.H., Wang, J.P. and Luo, H.L. (1994), “Crystallite size effect on saturation magnetization of fine ferrimagnetic particles”, *J. Magn. Magn. Mater.*, **136**(1-2), 176-182.
- Haw, C.Y., Mohamed, F., Chia, C.H., Radiman, S., Zakaria, S., Huang, N.M. and Lim, H.N. (2010), “Hydrothermal synthesis of magnetite nanoparticles as MRI contrast agents”, *Ceram. Int.*, **36**(4), 1417-1422.
- Hu, P., Yu, L., Zuo, A., Guo, C. and Yuan, F. (2009), “Fabrication of monodisperse magnetite hollow spheres”, *J. Phys. Chem. C*, **113**(3), 900-906.
- Huh, Y.M., Jun, Y.W., Song, H.T., Kim, S., Choi, J.S., Lee, J.H., Yoon, S., Kim, K.S., Shin, J.S., Suh, J.S. and Cheon, J. (2005), “In vivo magnetic resonance detection of cancer by using multifunctional magnetic nanocrystals”, *J. Am. Chem. Soc.*, **127**(35), 12387-12391.
- Iida, H., Takayanagi, K., Nakanishi, T. and Osaka, T. (2007), “Synthesis of Fe₃O₄ nanoparticles with various sizes and magnetic properties by controlled hydrolysis”, *J. Coll. Interf. Sci.*, **314**(1), 274-280.
- Jun, Y.W., Huh, Y.M., Choi, J.S., Lee, J.H., Song, H.T., Kim, S., Yoon, S., Kim, K.S., Shin, J.S., Suh, J.S. and Cheon, J. (2005), “Nanoscale size effect of magnetic nanocrystals and their utilization for cancer diagnosis via magnetic resonance imaging”, *J. Am. Chem. Soc.*, **127**(16), 5732-5733.
- Jung, H., Kim, J.W., Choi, H., Lee, J.H. and Hur, H.G. (2008), “Synthesis of nanosized biogenic magnetite and comparison of its catalytic activity in ozonation”, *Appl. Catal. B: Environ.*, **83**(3-4), 208-213.
- Kumar, S., Rajesh Raja, M., Manivel Mangalaraj, D., Viswanathan, C. and Ponpandian, N. (2013), “Surfactant free solvothermal synthesis of monodispersed 3D hierarchical Fe₃O₄ microspheres”, *Mater. Lett.* **110**, 98-101.
- Larumbe, S., Gómez Polo, C., Pérez Landazábal, J.I. and Pastor, J.M. (2012), “Effect of a SiO₂ coating on the magnetic properties of Fe₃O₄ nanoparticles”, *J. Phys.: Cond. Matter.*, **24**(26), 266007-266013.
- Legodi, M.A. and de Waal, D. (2007), “The preparation of magnetite, goethite, hematite and maghemite of pigment quality from mill scale iron waste”, *Dye. Pigmen.*, **74**(1), 161-168.
- Libert, S., Gorshkov, V., Goia, D., Matijevic, E. and Privman, V. (2003), “Model of controlled synthesis of uniform colloid particles: cadmium sulfide”, *Langimur*, **19**(26), 10679-10683.
- Liu, Z.L., Wang, X., Yao, K.L., Du, G.H., Lu, Q.H., Ding, Z.H., Tao, J., Ning, Q., Luo, X.P., Tian, D.Y. and Xi, D. (2004), “Synthesis of magnetite nanoparticles in W/O microemulsion”, *J. Mater. Sci.*, **39**(7),

- 2633-2636.
- Marchegiani, G., Imperatori, P., Mari, A., Pilloni, L., Chiolerio, A., Allia, P., Tiberto, P. and Suber, L. (2012), "Sonochemical synthesis of versatile hydrophilic magnetite nanoparticles", *Ultra. Sonochem.*, **19**(4), 877-882.
- Mascolo, M.C., Pei, Y. and Ring, T.A. (2013), "Room temperature co-precipitation synthesis of magnetite nanoparticles in a large pH window with different bases", *Mater.*, **6**(12), 5549-5567.
- Park, J., Lee, E., Hwang, N.M., Kang, M., Kim, S.C., Hwang, Y., Park, J.G., Noh, H.J., Kim, J.Y., Park, J.H. and Hyeon, T. (2005), "One-nanometer-scale size-controlled synthesis of monodisperse magnetic iron oxide nanoparticles", *Angew. Chem. Int. Ed.*, **44**(19), 2872-2877.
- Park, J., An, K., Hwang, Y., Park, J., Noh, H., Kim, J., Park, J., Hwang, N. and Hyeon, T. (2004), "Ultra-large-scale syntheses of monodisperse nanocrystals", *Nat. Mater.*, **3**, 891-895.
- Parkinson, G.S., Novotný, Z., Jacobson, P., Schmid, M. and Diebold, U. (2011), "Room temperature water splitting at the surface of magnetite", *J. Am. Chem. Soc.*, **133**(32), 12650-12655.
- Ravikumar, C. and Bandyopadhyaya, R. (2011), "Mechanistic study on magnetite nanoparticle formation by thermal decomposition and coprecipitation routes", *J. Phys. Chem. C*, **115**(5), 1380-1387.
- Roullin, V.G., Deverre, J.R., Lemaire, L., Hindre, F., Venier-Julienne, M.C., Vienet, R. and Benoit, J.P. (2002), "Anti-cancer drug diffusion within living rat brain tissue: an experimental study using [3H](6)-5-fluorouracil-loaded PLGA microspheres", *Eur. J. Pharm. Biopharm.*, **53**(3), 293-299.
- Sing, K.S.W., Everett, D.H., Haul, R.A.W., Moscou, L., Pierotty, R.A., Rouquerol, J. and Siemieniewska, T. (1985), "Reporting physisorption data for gas/solid systems. With special reference to determination of surface area and porosity (recommendations 1984)", *Pure Appl. Chem.*, **57**(4), 603-619.
- Song, Y., Wang, R., Rong, R., Ding, J., Liu, J., Li, R., Liu, Z., Li, H., Wang, X., Zhang, J. and Fang, J. (2011), "Synthesis of well-dispersed aqueous-phase magnetite nanoparticles and their metabolism as an MRI contrast agent for the reticuloendothelial system", *Eur. J. Inorg. Chem.*, **2011**(22), 3303-3313.
- Sun, X., Zheng, C., Zhang, F., Yang, Y., Wu, G., Yu, A. and Guan, N. (2009), "Size-controlled synthesis of magnetite (Fe₃O₄) nanoparticles coated with glucose and gluconic acid from a single Fe(III) precursor by a sucrose bifunctional hydrothermal method", *J. Phys. Chem. C*, **113**(36), 16002-16008.
- Wu, W., He, Q., Chen, H., Tang, J. and Nie, L. (2007), "Sonochemical synthesis, structure and magnetic properties of air-stable Fe₃O₄/Au nanoparticles", *Nanotech.*, **18**(14), 145609-145617.
- Xu, Z., Li, C., Kang, X., Yang, D., Yang, P., Hou, Z. and Lin, J. (2010), "Synthesis of a multifunctional nanocomposite with magnetic, mesoporous, and near-IR absorption properties", *J. Phys. Chem. C*, **114**(39), 16343-16350.
- Xuang, S., Wang, F., Lai, J.M.Y., Sham, K.W.Y., Wang, Y.X.J., Lee, S.F., Yu, J.C., Cheng, C.H.K. and Leung, K.C.F. (2011), "Synthesis of biocompatible, mesoporous Fe₃O₄ nano/microspheres with large surface area for magnetic resonance imaging and therapeutic application", *ACS Appl. Mater. Interf.*, **3**, 237-244.
- Yu, B.Y. and Kwak, S.Y. (2011), "Self-assembled mesoporous Co and Ni-ferrite spherical clusters consisting of spinel nanocrystals prepared using a template-free approach", *Dalton Trans.*, **40**(39), 9989-9998.
- Zhao, S.Y., Lee, D.K., Kim, C.W., Cha, H.G., Kim, Y.H. and Kang, Y.S. (2006), "Synthesis of magnetic nanoparticles of Fe₃O₄ and CoFe₂O₄ and their surface modification by surfactant adsorption", *Bull. Korean Chem. Soc.*, **27**(2), 237-242.
- Zhu, M. and Diao, G. (2011), "Synthesis of porous Fe₃O₄ nanospheres and its application for the catalytic degradation of xylenol orange", *J. Phys. Chem. C*, **115**(39), 18923-18934.